A stable and accurate shock-capturing hybrid FE-FD method

Tuan Anh Dao, Ken Mattsson & Murtazo Nazarov

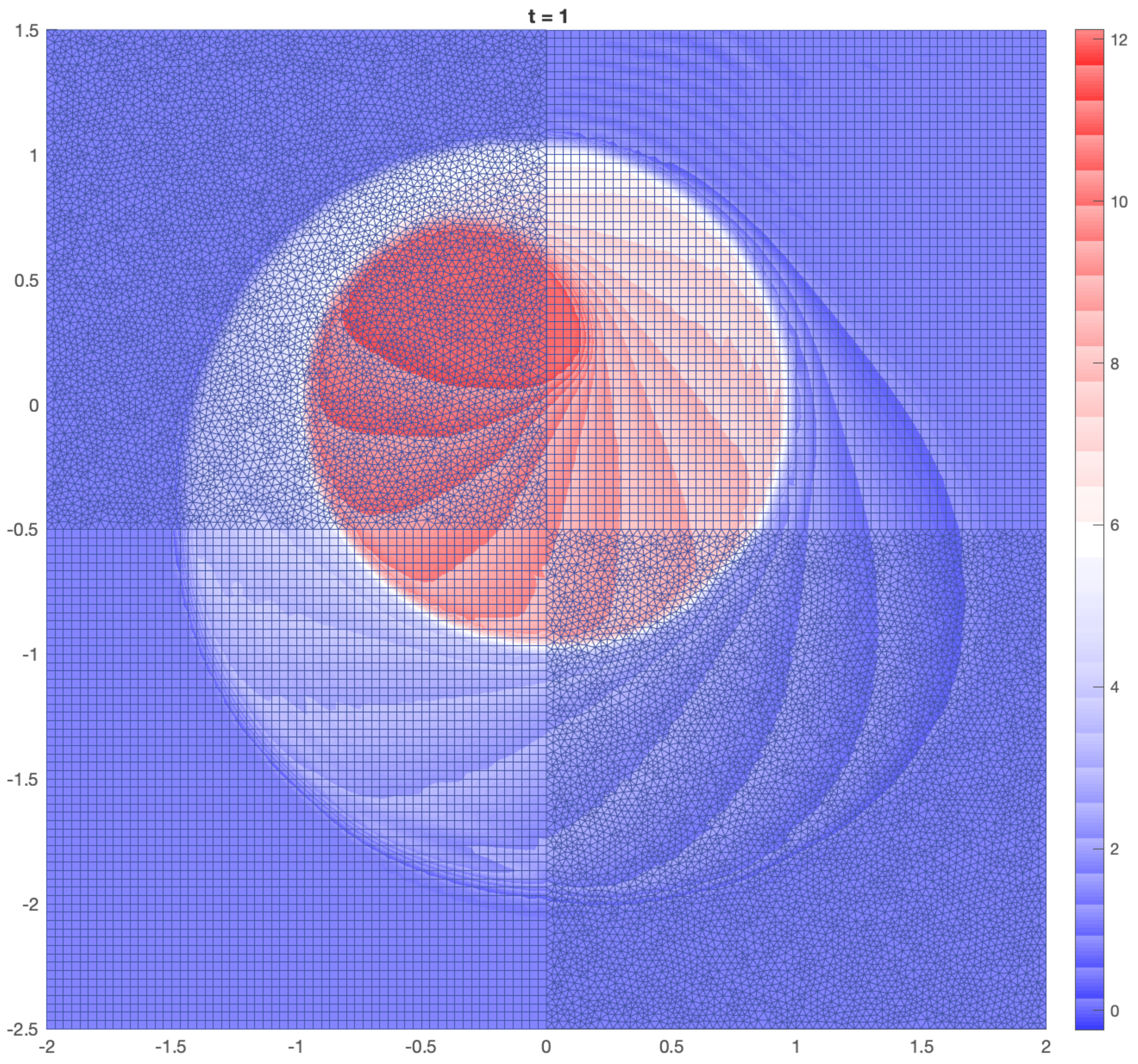

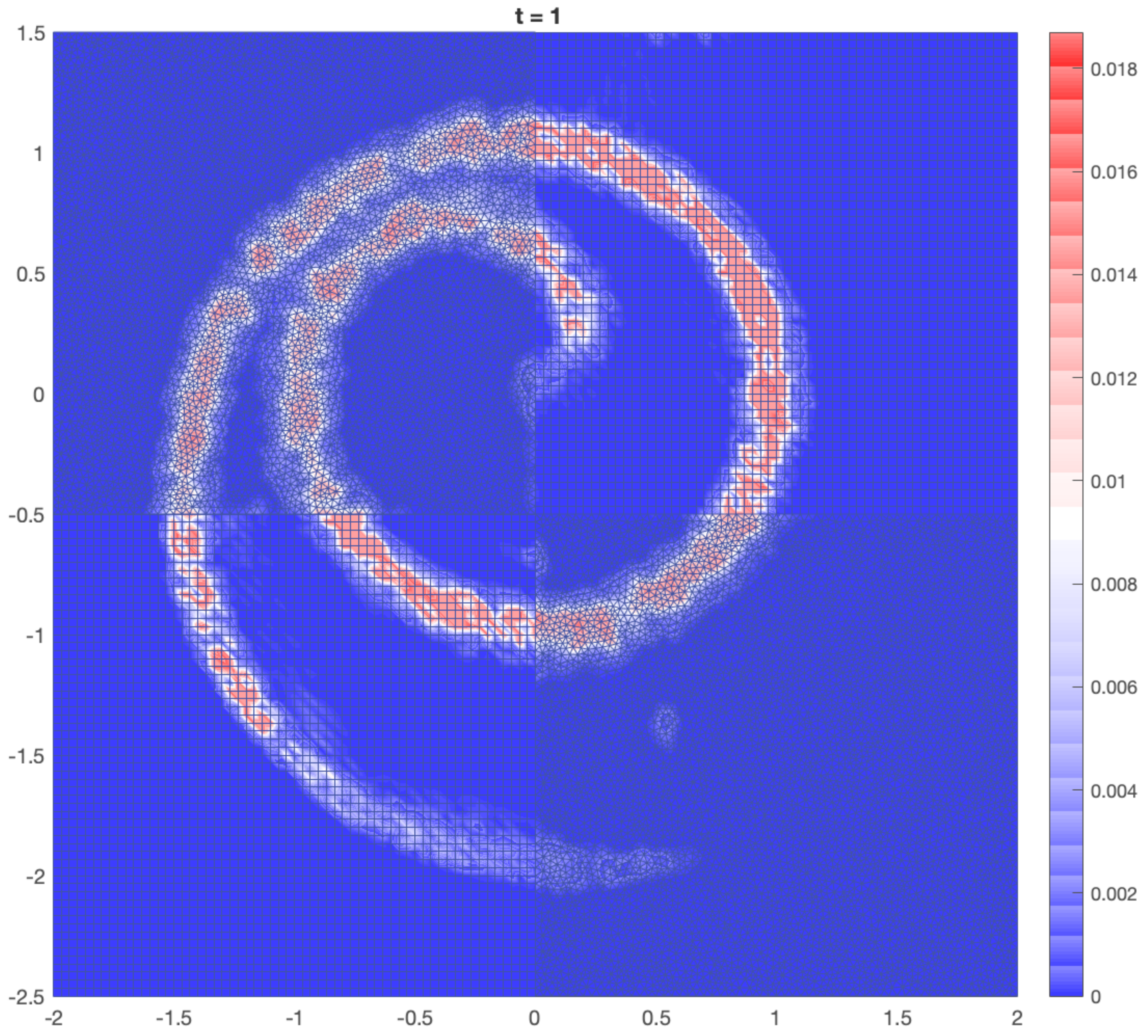

Tuan Anh Dao, TDB Seminar May 25th 2020

Two well-known numerical methods for PDEs

Finite difference (FD) methods:
- ease of using high order stencils
- less storage & computation
- logically structured mesh

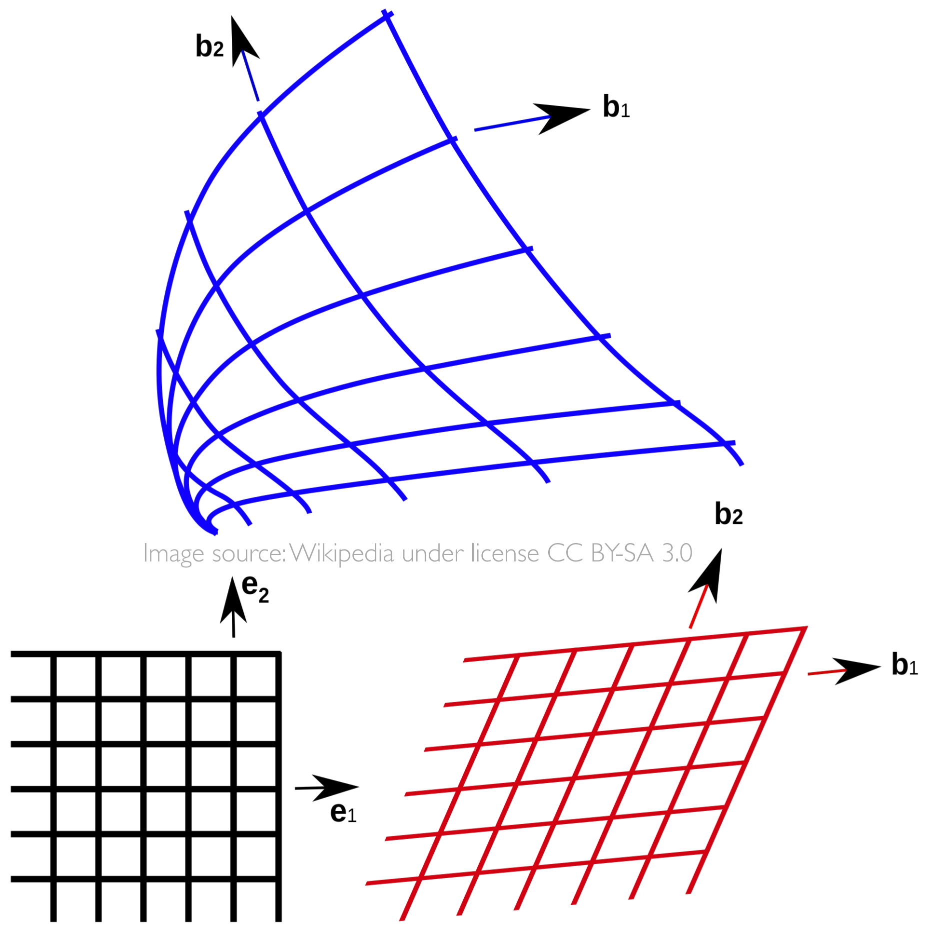

Hybrid FE-FD method

Finite element (FE) methods:
- complex geometries
- mathematical reliability
- more storage
- more computation

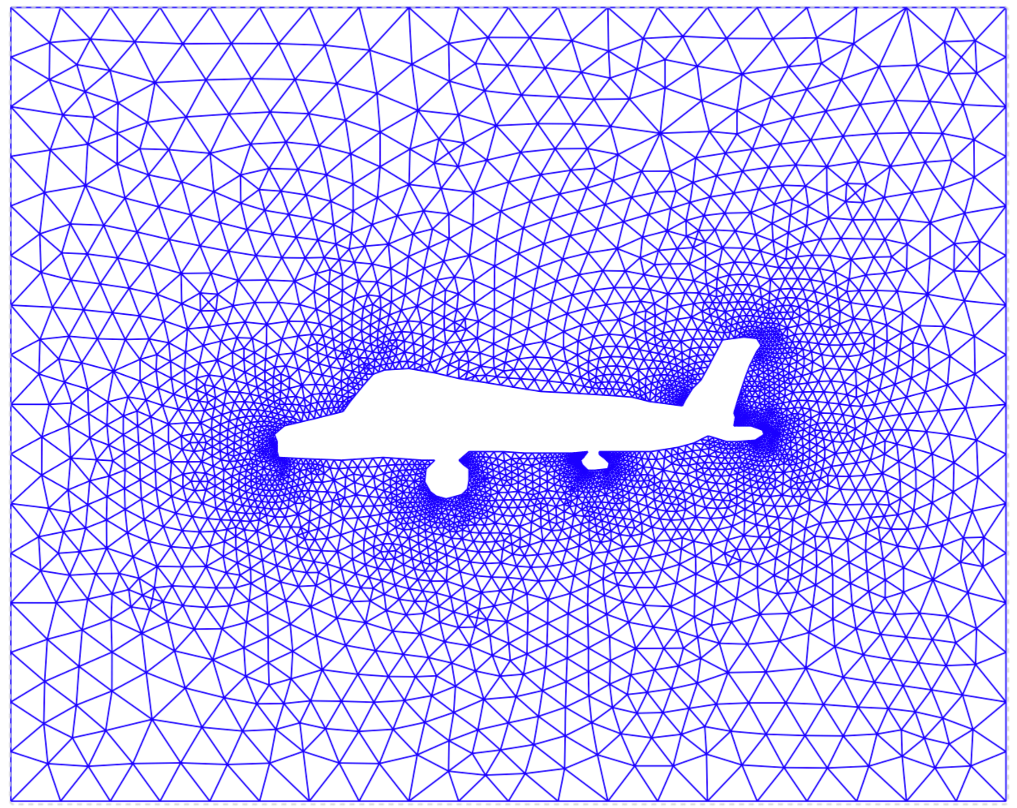

Aim: Computational efficiency
on realistic geometries

Simple practical scenarios

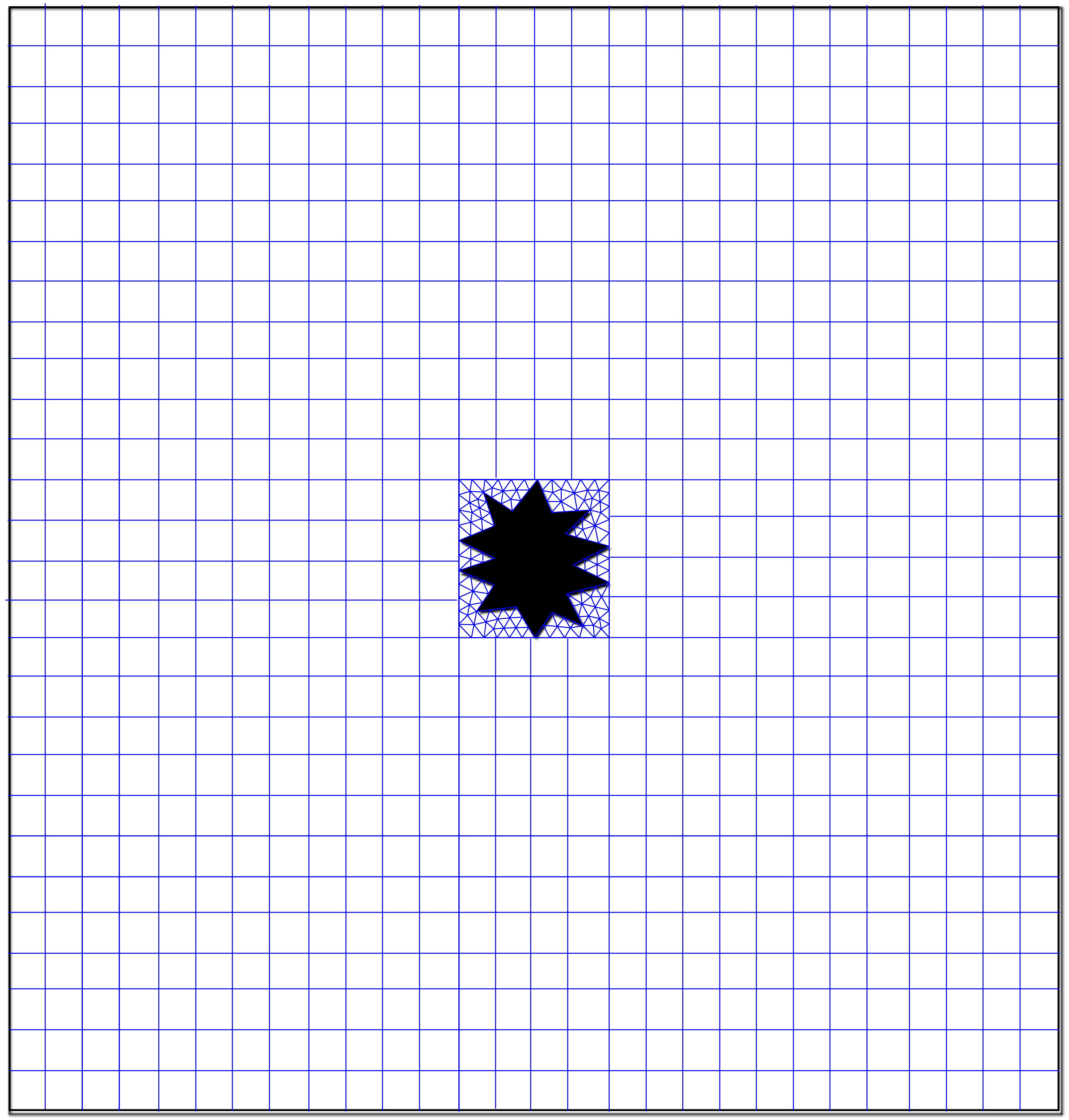

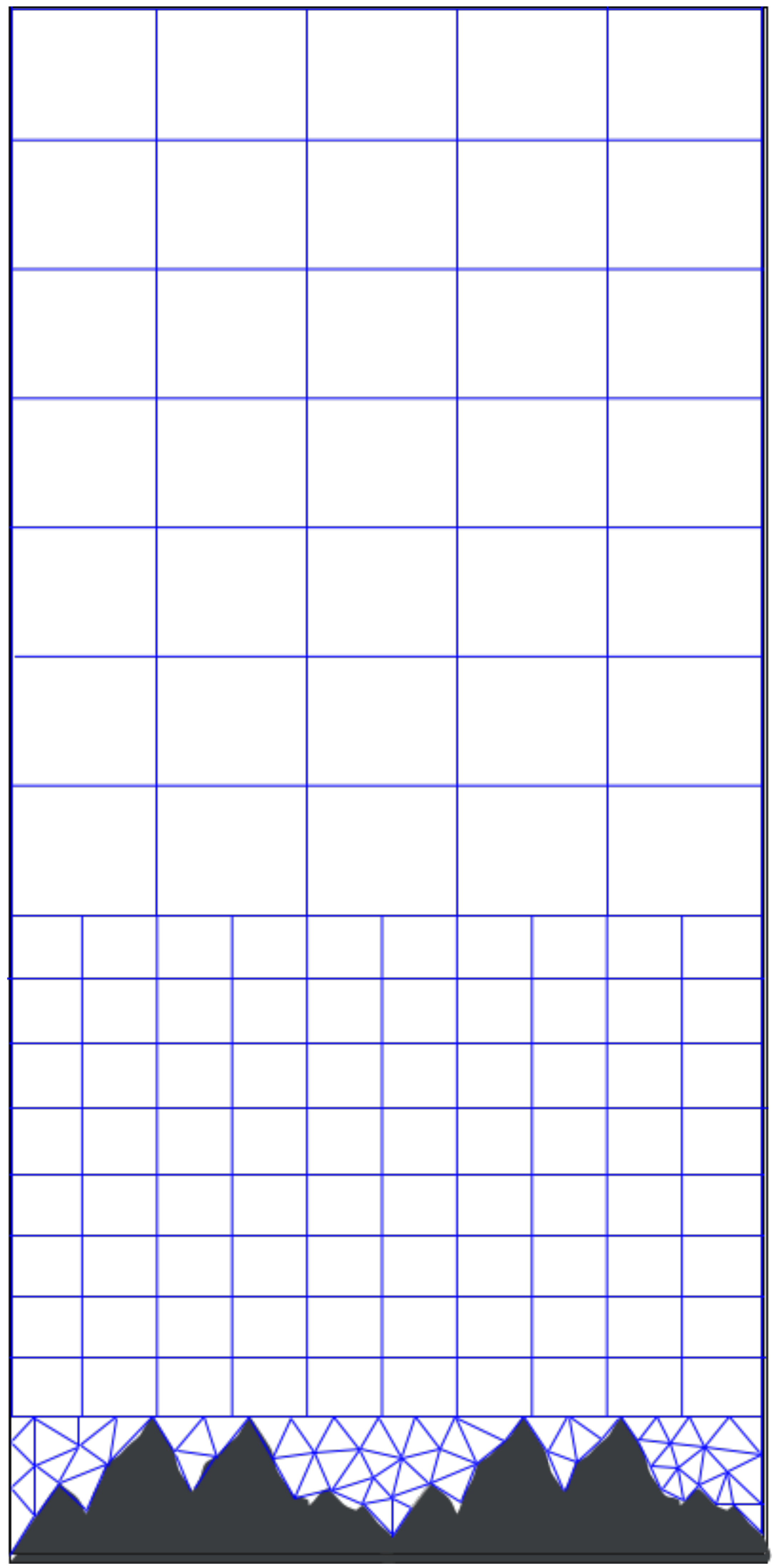

Other works

- Seismology *[Galis et al. 2008]*, [*Ma et al. 2004]*
  Transition region with averaging solution: No stability control, requiring diagonal or lumped mass matrix.

- Electrical modeling *[Vachiratienchai et al. 2010]*
  At areas of interest, each FD rectangular block is splitted into two FE elements resulting in modified schemes. No stability control, unstable if splitting angle is too large/small.

- Summation-By-Parts (SBP) coupling: FD-FD *[Mattsson & Carpenter 2010]*, FD-DG *[Kozdon & Wilcox 2016]*, FD-FV *[Lundquist et al. 2018].*
  All use diagonal norms, linear problems.

The coupling Simultaneous-Approximation-Terms (SAT) technique

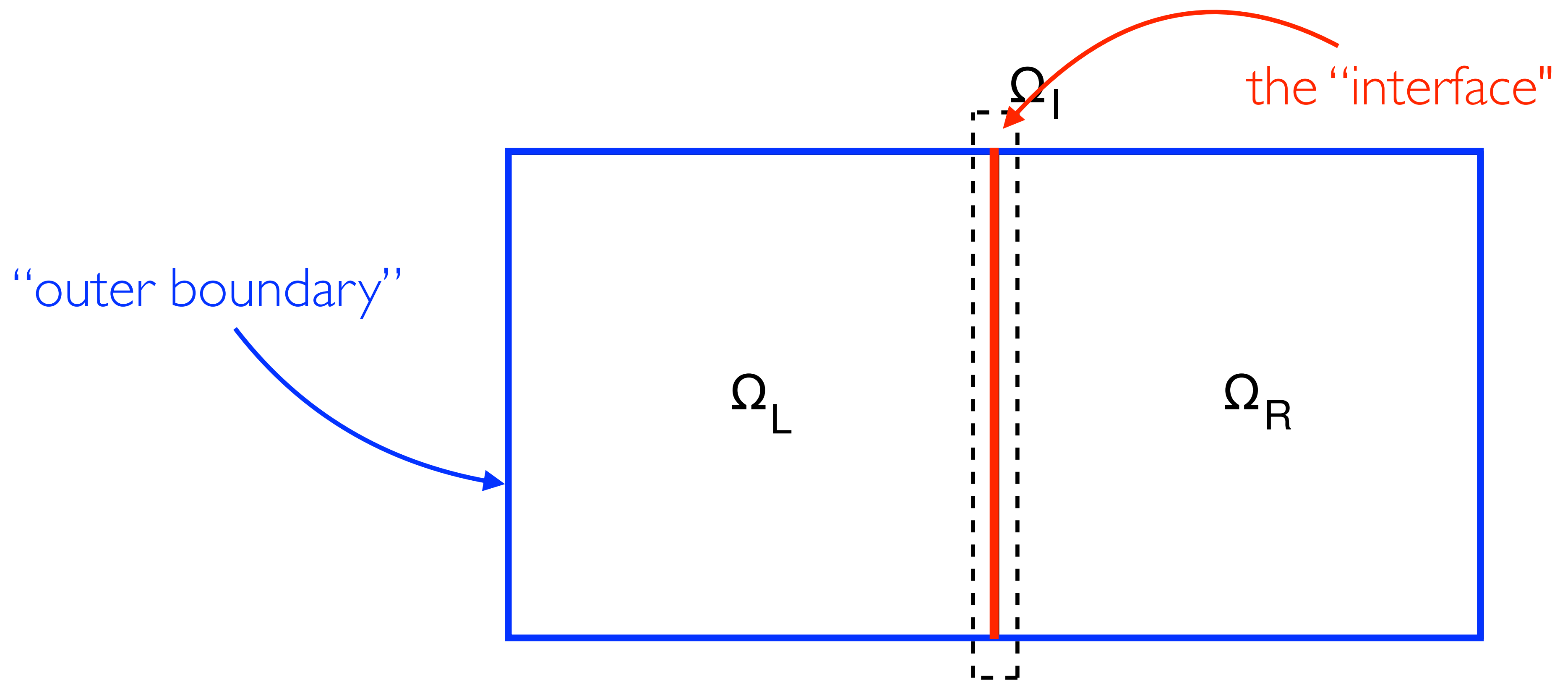

$$u_t + \nabla \cdot \mathbf{f}(u) = \nabla \cdot \big(\epsilon(x,y)\nabla u\big), x \in \Omega_L$$
$$v_t + \nabla \cdot \mathbf{f}(v) = \nabla \cdot \big(\epsilon(x,y)\nabla v\big), x \in \Omega_R$$

consider a general conservation law

weakly enforce outer BCs

$$\mathbf{u}_t + \mathcal{H}_L^{-1}\mathcal{Q}_L\hat{\mathbf{f}}(\mathbf{u}) = \mathcal{H}_L^{-1}\mathcal{R}_L^{(\epsilon)}\mathbf{u} + \boxed{\mathrm{SAT}_L} + \boxed{\mathrm{SAT}_{IL}}$$
$$\mathbf{v}_t + \mathcal{H}_R^{-1}\mathcal{Q}_R\hat{\mathbf{f}}(\mathbf{v}) = \mathcal{H}_R^{-1}\mathcal{R}_R^{(\epsilon)}\mathbf{v} + \boxed{\mathrm{SAT}_R} + \boxed{\mathrm{SAT}_{IR}}$$

weakly enforce interface continuity conditions

Accuracy and Stability conditions

Continuity condition on Ω_I

$$u = v$$

$$u_x = v_x$$

continuous settings

$$\mathbf{u} = \mathbf{v}\,, \qquad \hat{\mathbf{f}}(\mathbf{u}) = \hat{\mathbf{f}}(\mathbf{v})$$

$$\mathbf{u}_x = \mathbf{v}_x\,, \qquad \hat{\mathbf{f}}_x(\mathbf{u}) = \hat{\mathbf{f}}_x(\mathbf{v})$$

discrete settings

forcing weakly using SAT

Accuracy $\mathbf{u}_I = I_{R2L}\mathbf{v}_I + \mathcal{O}(h^p), \quad \mathbf{v}_I = I_{L2R}\mathbf{u}_I + \mathcal{O}(h^p)$

SBP-preserving $I_{R2L}^T \mathcal{H}^y_L = \mathcal{H}^y_R I_{L2R}$

$$I_{R2L}^T \mathcal{H}^y_L = M_I I_{L2R}, \quad M_I = \int_{\Omega_I} \varphi_j \varphi_i ds$$

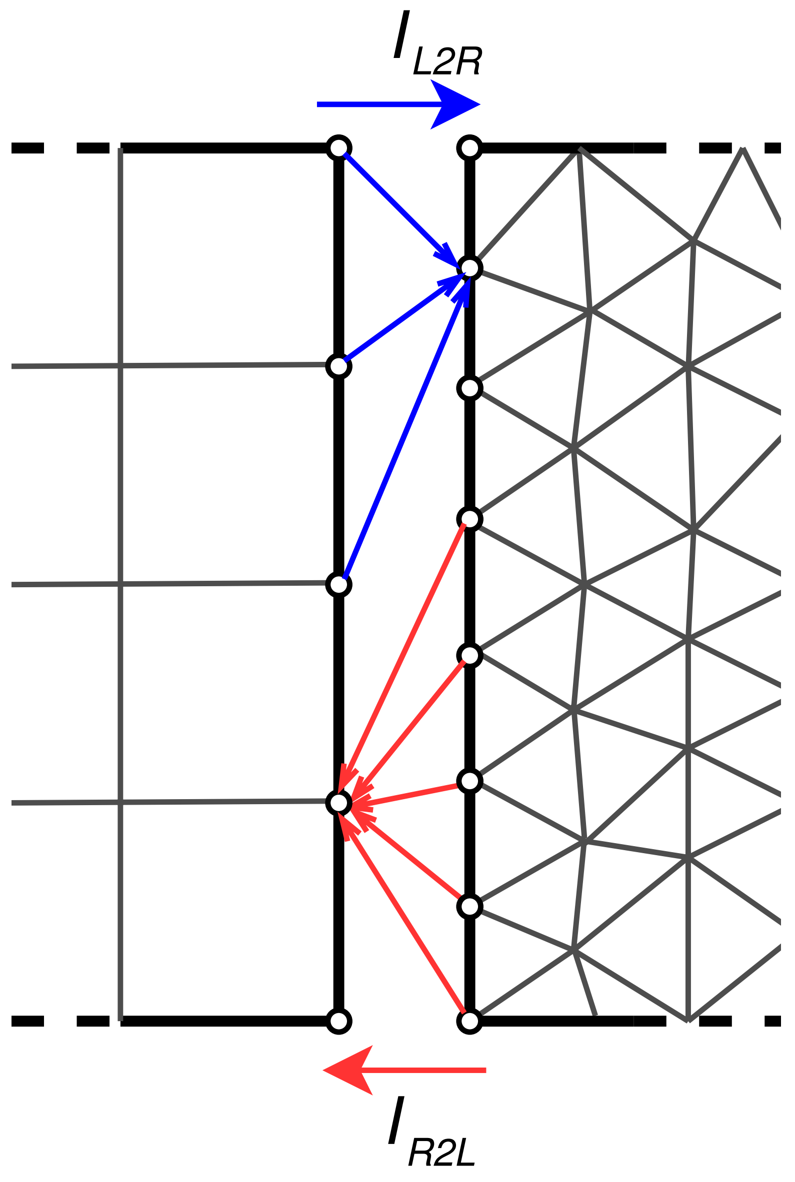

The coupling SAT technique

1 Based on a skew-symmetric splitting of the flux

Skew-symmetric splitting $\nabla \cdot \mathbf{f} = (\alpha \nabla) \cdot \mathbf{f} + \mathbf{f}'(u) \cdot \left(\tilde{\alpha}\, \nabla\right) u, \quad \alpha \in \mathbb{R}^2, \tilde{\alpha} = 1 - \alpha$ such that no energy changes happen from the interior domain

With a choice of penalty parameters, energy terms are cancelled

$\mathbf{u} = \mathbf{v}\,, \qquad \hat{\mathbf{f}}(\mathbf{u}) = \hat{\mathbf{f}}(\mathbf{v})$

$\mathbf{u}_x = \mathbf{v}_x\,, \qquad \hat{\mathbf{f}}_x(\mathbf{u}) = \hat{\mathbf{f}}_x(\mathbf{v})$

depending on α

→ **Energy conservation**

2 Characteristic coupling

Let $\mathbf{f}'_+ = \dfrac{\mathbf{f}' + |\mathbf{f}'|}{2}, \quad \mathbf{f}'_- = \dfrac{\mathbf{f}' - |\mathbf{f}'|}{2}$

Forcing $\mathbf{f}'_-(\mathbf{u})(\mathbf{u} - \mathbf{v}) = 0$ yields $\dfrac{d}{dt}||\mathbf{u}||^2 + \dfrac{d}{dt}||\mathbf{v}||^2 \leq 0$

$\mathbf{f}'_+(\mathbf{v})(\mathbf{v} - \mathbf{u}) = 0$

→ **Energy damping, more robust**

Nondiagonal-norm SBP-preserving interpolation operators

1 Based on structure of the interpolation matrices

$$I_{R2L} = \begin{bmatrix}
q_{1,1} & \cdots & & & & & & \cdots & q_{1,r} & & & & & & \\
\vdots & & & & & & & & \vdots & & & & & & \\
q_{t,1} & \cdots & & & & & & \cdots & q_{t,r} & & & & & & \\
 & & q_{2s} & q_{2s-1} & \cdots & q_0 & \cdots & q_{2s-1} & q_{2s} & & & & & & \\
 & & & q_{2s} & q_{2s-1} & \cdots & q_0 & \cdots & q_{2s-1} & q_{2s} & & & & & \\
 & & & & \ddots & \ddots & \ddots & \ddots & \ddots & \ddots & & & & & \\
 & & & & & q_{2s} & q_{2s-1} & \cdots & q_0 & \cdots & q_{2s-1} & q_{2s} & & & \\
 & & & & & & q_{2s} & q_{2s-1} & \cdots & q_0 & \cdots & q_{2s-1} & q_{2s} & & \\
 & & & & & & q_{t,r} & \cdots & & & & & & \cdots & q_{t,1} \\
 & & & & & & \vdots & & & & & & & & \vdots \\
 & & & & & & q_{1,r} & \cdots & & & & & & \cdots & q_{1,1}
\end{bmatrix}, \quad I_{L2R} = H^{-1}(M_I I_{R2L})^T$$

For example, 6th order FD - P1 FE,

$r = 18, t = 6, s = 7$

2 From existing diagonal norm interpolation operators

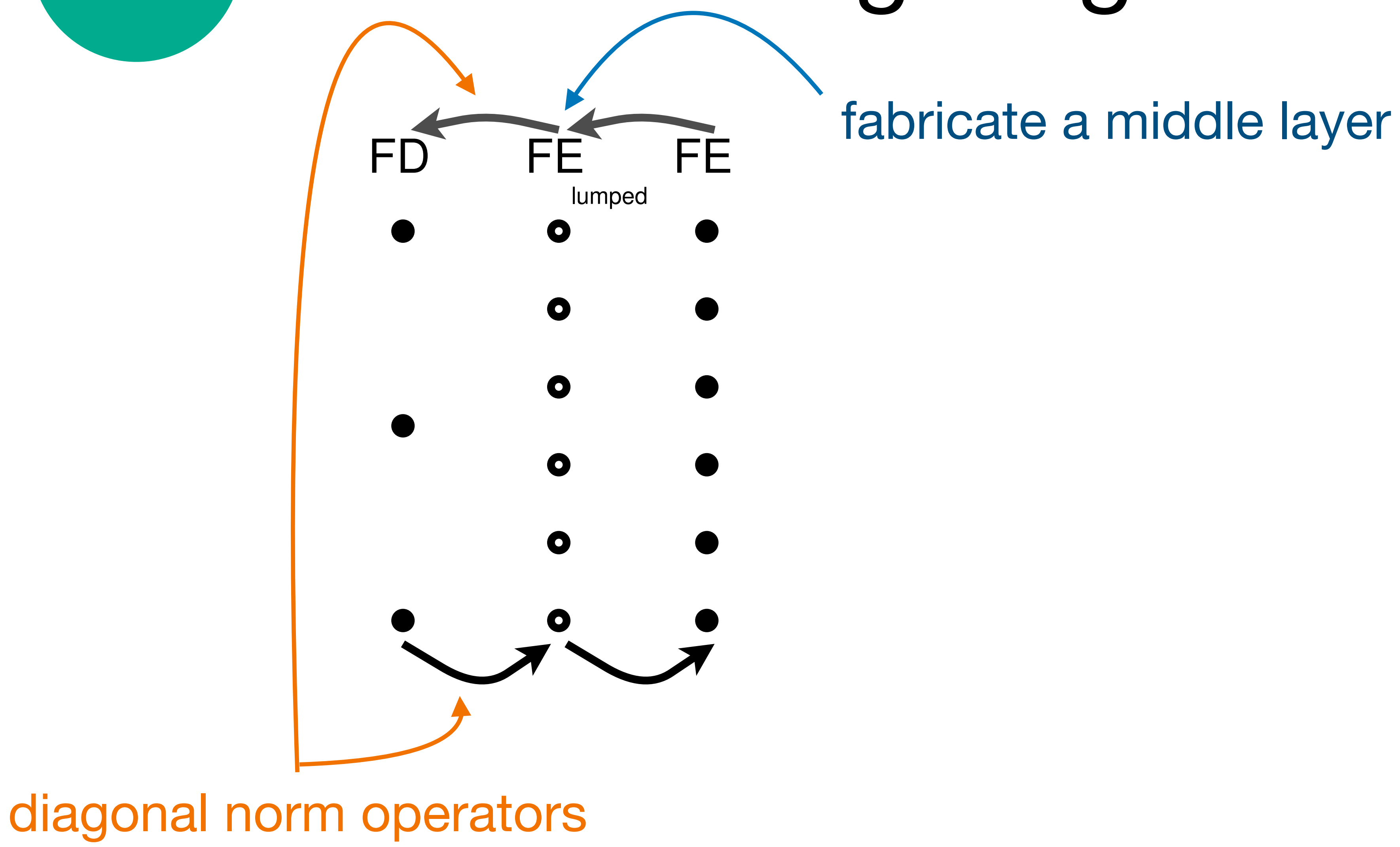

Construct $I_{L2R} = I_{M2R} I_{L2M}$ and $I_{R2L} = I_{M2L} I_{R2M}$

For $\mathbb{P}^1$ FE $I_{M2R} = I_{m\times n}, I_{R2M} = (M_I H^{-1})^T$

A residual-based viscosity stabilization

Residual

$$R(\mathbf{u}) = D_t\mathbf{u} + D_f\mathbf{u}, \quad D_t\mathbf{u} \approx u_t, \quad D_f\mathbf{u} \approx \nabla \cdot \mathbf{f}(u)$$

Artificial viscosity

$$\varepsilon_a = \min\left(C_{vel}h\,|\,\mathbf{f}'(\mathbf{u})\,|\,, C_{rv}h^2 \frac{\max_{loc}||R(\mathbf{u})||}{n(\mathbf{u})}\right)$$

where $n(\mathbf{u}) = ||\mathbf{u} - \bar{\mathbf{u}}||_{\infty,\Omega}$ is a normalization term

Set $\varepsilon = \max(\varepsilon_a, \varepsilon_p)$ physical viscosity

The amount of artificial viscosity on each part of the domain can be (very) different.

Instead of $u_x = v_x$, couple $\varepsilon_L u_x = \varepsilon_R v_x$

amount of viscosity on the left and right domains $\longrightarrow$ Allows jumps on the physical viscosity! (discontinuous media)

Numerical results

Linear advection-diffusion

$$u_t + a^T \nabla u = \epsilon \nabla^T \nabla u, x \in \Omega_L$$
$$v_t + a^T \nabla v = \epsilon \nabla^T \nabla v, x \in \Omega_R$$

SBP discretization

$$\mathbf{u}_t + \mathscr{H}_L^{-1} \mathscr{Q}_L \mathbf{u} = \epsilon \mathscr{H}_L^{-1} \mathscr{R}_L \mathbf{u} + \mathrm{SAT}_L + \mathrm{SAT}_{IL}$$
$$\mathbf{v}_t + \mathscr{H}_R^{-1} \mathscr{Q}_R \mathbf{v} = \epsilon \mathscr{H}_R^{-1} \mathscr{R}_R \mathbf{v} + \mathrm{SAT}_R + \mathrm{SAT}_{IR}$$

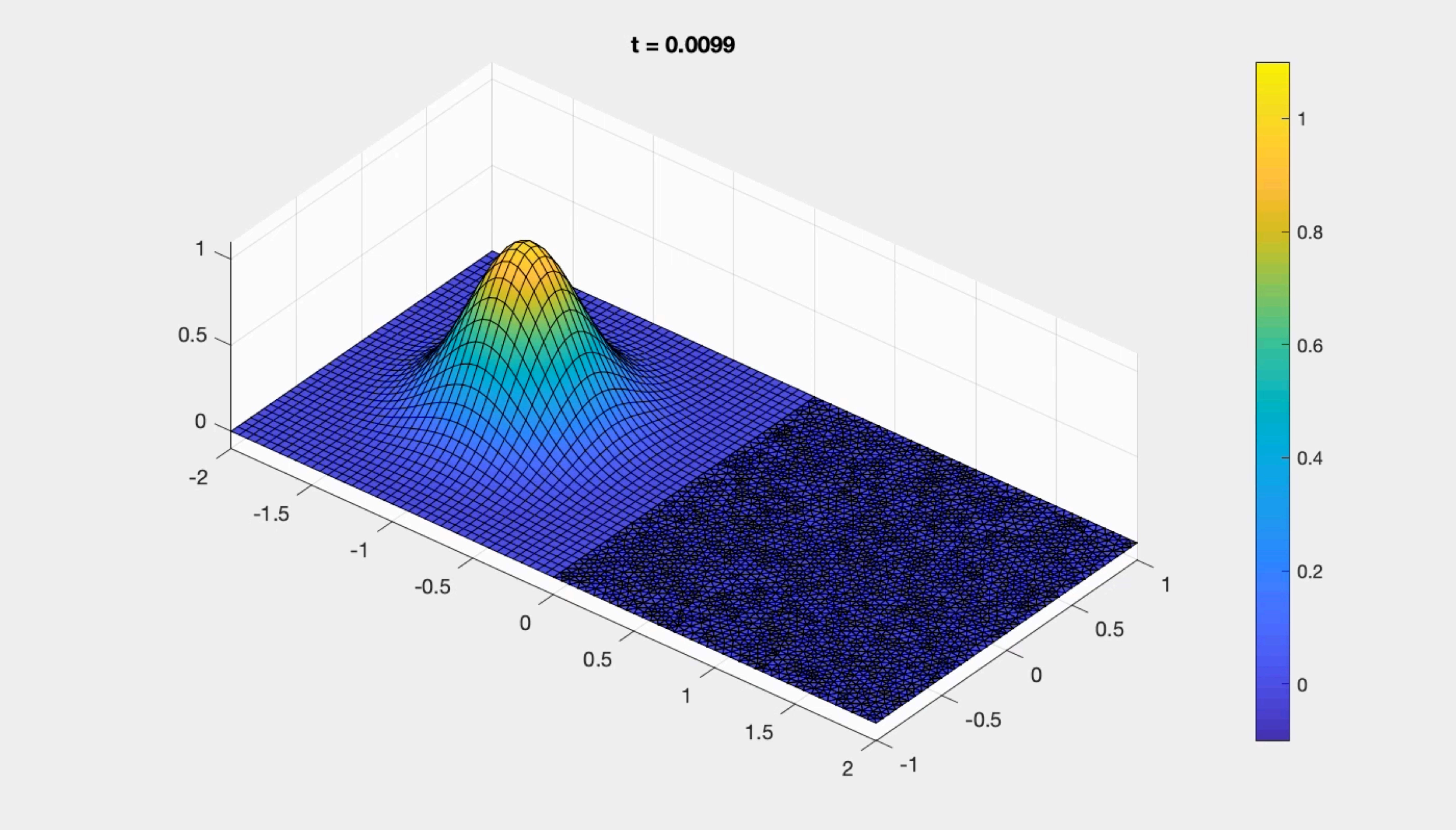

Numerical results

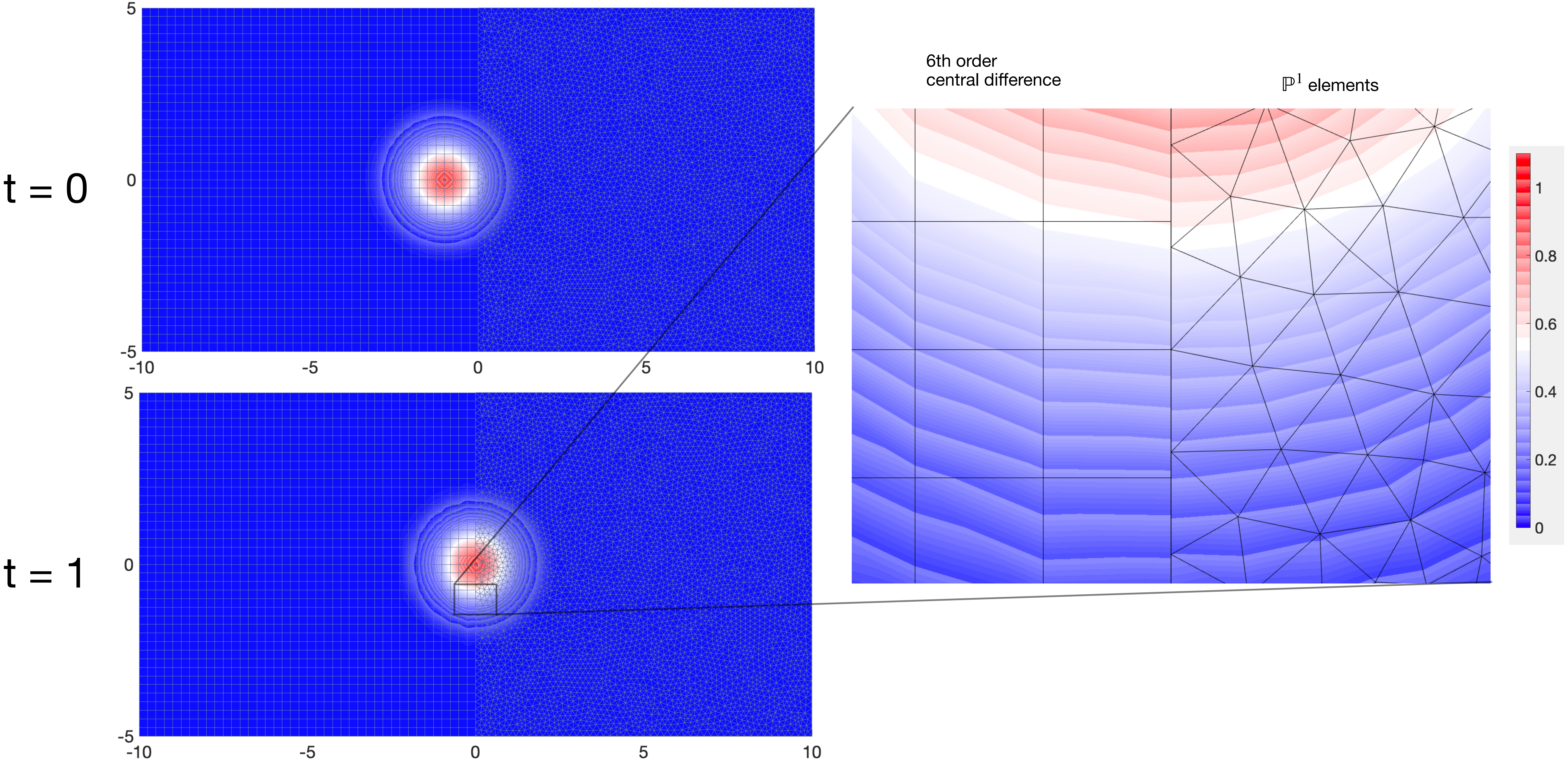

Numerical results - Eigenvalue analysis

Semi-discrete form $\begin{bmatrix} u \\ v \end{bmatrix}_t = F \times \begin{bmatrix} u \\ v \end{bmatrix}$

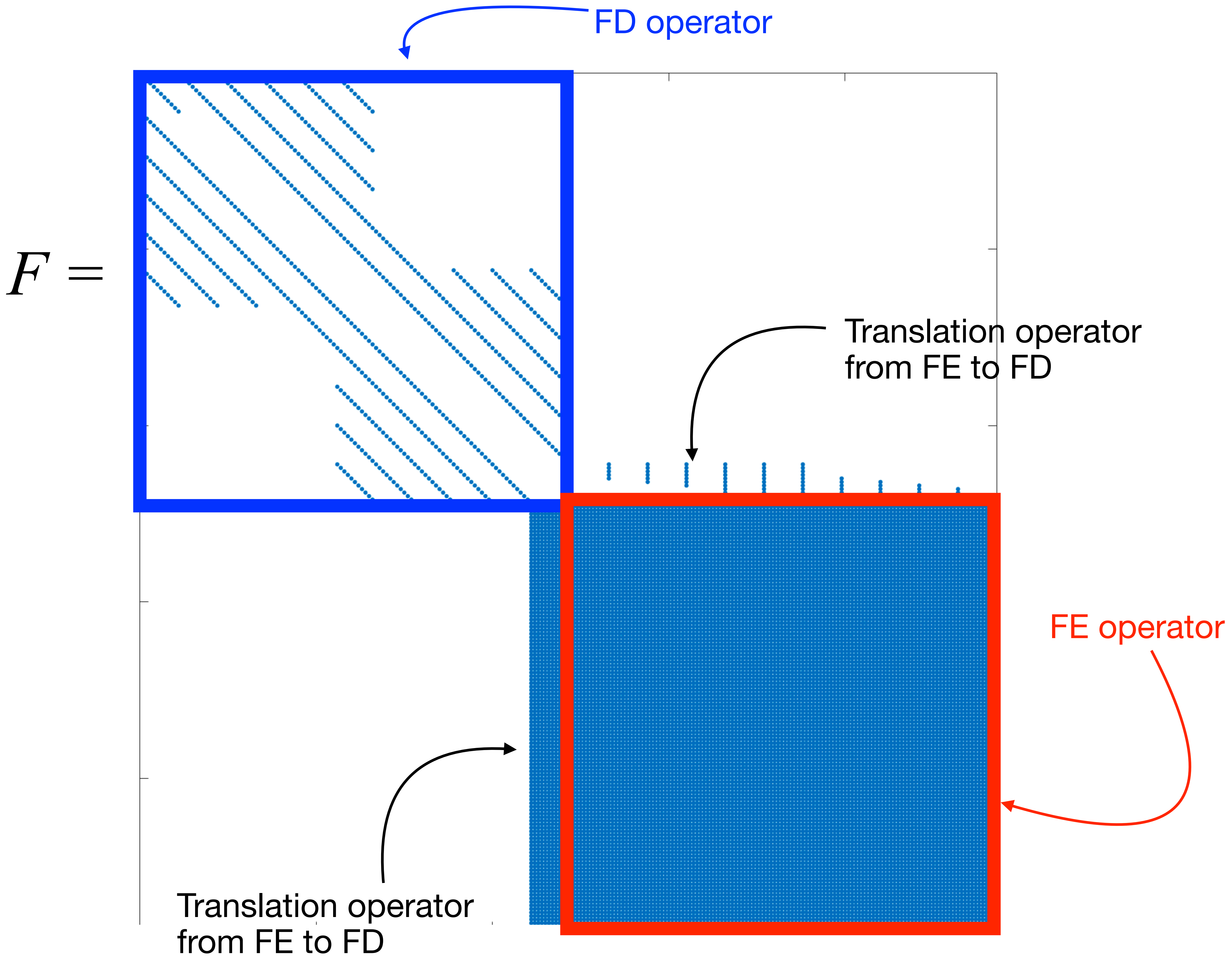

Matlab: spy(F)

Eigenvalues on complex plane

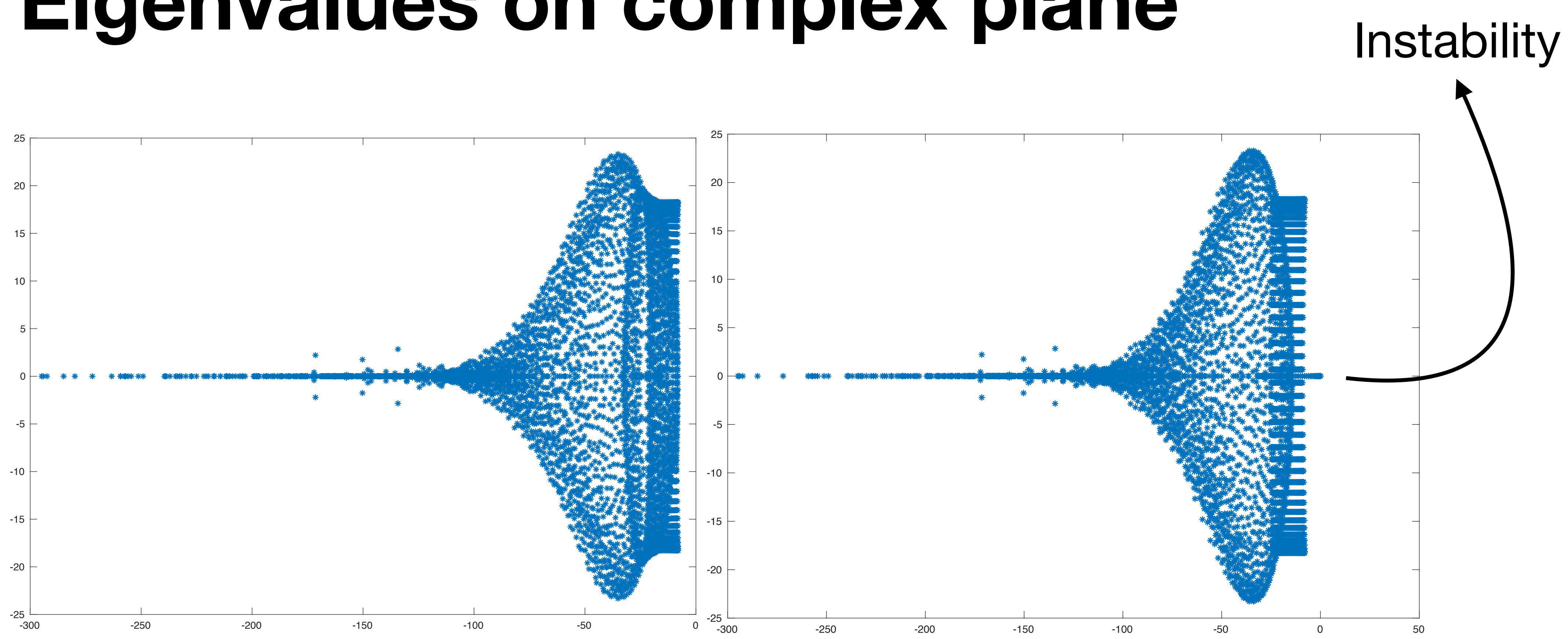

With interface treatment **Without** interface treatment

(Both are with proper outer boundary treatment)

Numerical results - Convergence

$a = (\pm 1{,}0)^T, \epsilon = 0.01$ (viscous)

m	2^{nd} order FD to P^1 FE				4^{th} order FD to P^1 FE			
	$\log_{10}(l_2(u))$	$\log_{10}(l_2(v))$	$\log_{10}(l_2(u)+l_2(v))$	Q	$\log_{10}(l_2(u))$	$\log_{10}(l_2(v))$	$\log_{10}(l_2(u)+l_2(v))$	Q
31	-4.16	-2.29	-2.29	–	-4.85	-3.25	-3.24	–
41	-5.46	-2.56	-2.56	2.15	-5.60	-3.59	-3.59	2.80
51	-5.27	-2.76	-2.76	2.06	-6.12	-3.82	-3.82	2.43
61	-5.32	-2.92	-2.92	2.01	-6.52	-4.00	-4.00	2.24

From FD to FE, matching interface

m	P^1 FE to 2^{nd} order FD				P^1 FE to 4^{th} order FD			
	$\log_{10}(l_2(u))$	$\log_{10}(l_2(v))$	$\log_{10}(l_2(u)+l_2(v))$	Q	$\log_{10}(l_2(u))$	$\log_{10}(l_2(v))$	$\log_{10}(l_2(u)+l_2(v))$	Q
31	-2.32	-5.92	-2.32	–	-2.93	-5.75	-2.93	–
41	-2.56	-6.08	-2.56	1.94	-3.19	-6.09	-3.19	2.11
51	-2.75	-6.23	-2.75	1.96	-3.39	-6.28	-3.39	2.02
61	-2.91	-6.37	-2.91	1.97	-3.55	-6.42	-3.55	1.99

From FE to FD, matching interface

m_L	m_R	2^{nd} order FD to P^1 FE				4^{th} order FD to P^1 FE			
		$\log_{10}(l_2(u))$	$\log_{10}(l_2(v))$	$\log_{10}(l_2(u)+l_2(v))$	Q	$\log_{10}(l_2(u))$	$\log_{10}(l_2(v))$	$\log_{10}(l_2(u)+l_2(v))$	Q
21	41	-2.69	-1.92	-1.86	–	-3.62	-2.75	-2.69	–
31	61	-4.14	-2.29	-2.28	2.42	-4.87	-3.40	-3.39	3.95
41	81	-5.45	-2.56	-2.56	2.17	-5.57	-3.86	-3.86	3.74

From FD to FE, nonmatching interface

m_L	m_R	P^1 FE to 2^{nd} order FD				P^1 FE to 4^{th} order FD			
		$\log_{10}(l_2(u))$	$\log_{10}(l_2(v))$	$\log_{10}(l_2(u)+l_2(v))$	Q	$\log_{10}(l_2(u))$	$\log_{10}(l_2(v))$	$\log_{10}(l_2(u)+l_2(v))$	Q
21	41	-2.00	-4.43	-2.00	–	-2.73	-4.12	-2.72	–
31	61	-2.32	-6.23	-2.32	1.84	-3.34	-6.35	-3.34	3.54
41	81	-2.56	-6.49	-2.56	1.94	-3.71	-6.64	-3.71	2.96

From FE to FD, nonmatching interface

$a = (\pm 1{,}0)^T, \epsilon = 0$ (inviscid)

m	2^{nd} order FD to P^1 FE				4^{th} order FD to P^1 FE			
	$\log_{10}(l_2(u))$	$\log_{10}(l_2(v))$	$\log_{10}(l_2(u)+l_2(v))$	Q	$\log_{10}(l_2(u))$	$\log_{10}(l_2(v))$	$\log_{10}(l_2(u)+l_2(v))$	Q
31	-1.72	-1.10	-1.01	–	-1.71	-1.73	-1.42	
41	-2.05	-1.30	-1.23	1.78	-2.15	-2.12	-1.83	3.28
51	-2.26	-1.48	-1.41	1.90	-2.54	-2.43	-2.18	3.58
61	-2.42	-1.63	-1.57	1.97	-2.83	-2.67	-2.44	3.26

From FD to FE

m	P^1 FE to 2^{nd} order FD				P^1 FE to 4^{th} order FD			
	$\log_{10}(l_2(u))$	$\log_{10}(l_2(v))$	$\log_{10}(l_2(u)+l_2(v))$	Q	$\log_{10}(l_2(u))$	$\log_{10}(l_2(v))$	$\log_{10}(l_2(u)+l_2(v))$	Q
31	-1.12	-1.69	-1.01	–	-1.73	-1.72	-1.43	–
41	-1.31	-2.06	-1.24	1.80	-2.12	-2.17	-1.84	3.32
51	-1.49	-2.31	-1.43	1.94	-2.43	-2.57	-2.20	3.67
61	-1.64	-2.50	-1.59	2.00	-2.67	-2.89	-2.47	3.40

From FE to FD

Remark: *superconvergence* is preserved!

The FE advection operator using piecewise linear basis functions is fourth order with a regular mesh if the error is measured by $\sqrt{e^T \mathbf{M} e}$ (see [Andreev,1988])

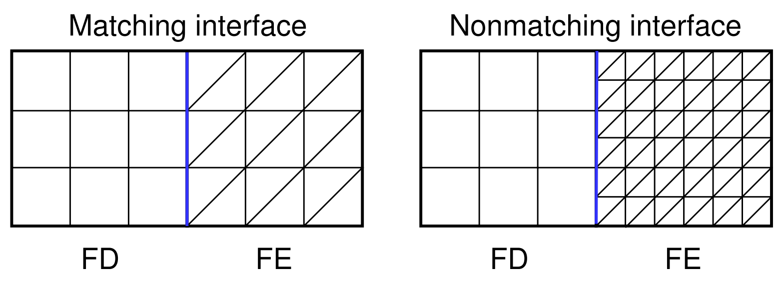

Numerical results - Convergence

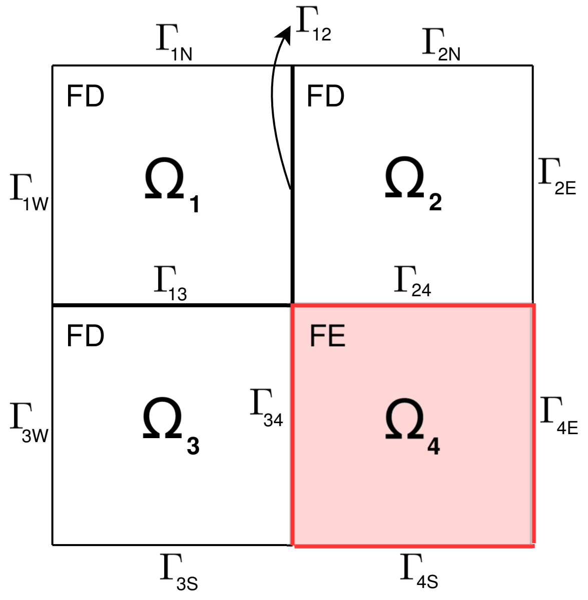

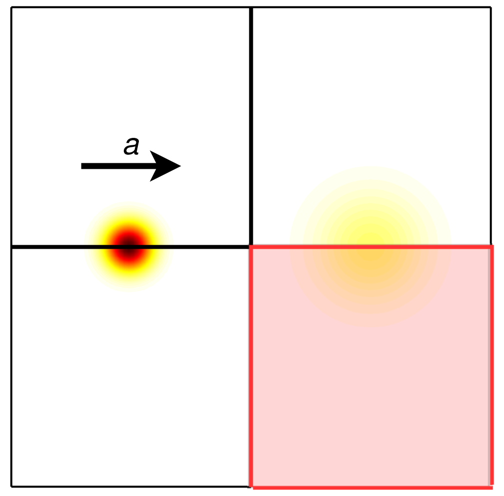

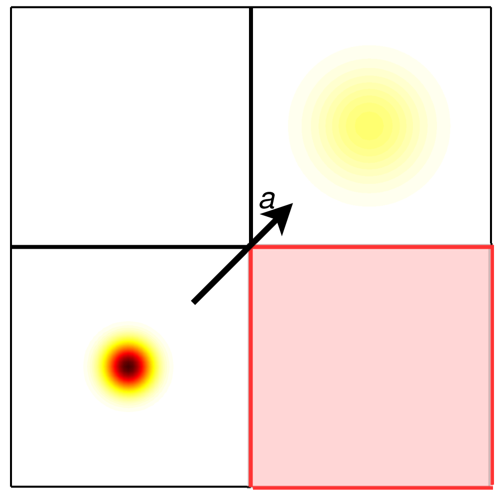

Nonmatching Test case (b), Delaunay triangulated mesh, Fourth-order FD, $\mathbb{P}^1$ FE, $\boldsymbol{a} = (1,0)^T, x_0 = -1, y_0 = 0, T = 2$

m (FD)	$r_{\max}$ (FE)	inviscid $\varepsilon = 0$				viscous $\varepsilon = 0.01$			
		$l_2e(\boldsymbol{u}_{FD})$	$l_2e(\boldsymbol{u}_{FE})$	$l_2e(\boldsymbol{u})$	Q	$l_2e(\boldsymbol{u}_{FD})$	$l_2e(\boldsymbol{u}_{FE})$	$l_2e(\boldsymbol{u})$	Q
21	D/41	1.54E-1	3.39E-2	1.86E-1	–	3.31E-2	1.55E-2	4.90E-2	–
26	D/51	9.55E-2	2.00E-2	1.15E-1	2.20	2.45E-2	1.74E-2	4.17E-2	0.65
31	D/61	5.88E-2	1.17E-2	7.08E-2	2.67	1.48E-2	1.17E-2	2.69E-2	2.47
36	D/71	3.71E-2	7.41E-3	4.47E-2	3.00	9.33E-3	7.76E-3	1.70E-2	2.93
41	D/81	2.45E-2	5.01E-3	2.95E-2	3.09	5.62E-3	4.90E-3	1.05E-2	3.57
46	D/91	1.73E-2	3.39E-3	2.04E-2	3.05	3.31E-3	3.02E-3	6.31E-3	4.30

Nonmatching Test case (c), Delaunay triangulated mesh, Fourth-order FD, $\mathbb{P}^1$ FE, $\boldsymbol{a} = (1,1)^T, x_0 = -1, y_0 = -1, T = 2$

m (FD)	$r_{\max}$ (FE)	inviscid $\varepsilon = 0$				viscous $\varepsilon = 0.01$			
		$l_2e(\boldsymbol{u}_{FD})$	$l_2e(\boldsymbol{u}_{FE})$	$l_2e(\boldsymbol{u})$	Q	$l_2e(\boldsymbol{u}_{FD})$	$l_2e(\boldsymbol{u}_{FE})$	$l_2e(\boldsymbol{u})$	Q
21	D/41	1.91E-1	5.25E-2	2.40E-1	–	2.40E-2	1.58E-3	2.57E-2	–
26	D/51	1.29E-1	3.09E-2	1.58E-1	1.88	9.33E-3	4.90E-5	9.33E-3	4.50
31	D/61	8.71E-2	1.62E-2	1.05E-1	2.37	4.68E-3	1.95E-6	4.68E-3	3.82
36	D/71	5.89E-2	1.00E-2	6.92E-2	2.69	2.69E-3	1.07E-6	2.69E-3	3.60
41	D/81	3.89E-2	6.76E-3	4.57E-2	3.03	1.66E-3	2.24E-7	1.66E-3	3.70
46	D/91	2.88E-2	3.98E-3	3.24E-2	2.83	1.05E-3	1.05E-7	1.05E-3	3.79

Numerical results - The KPP problem $\mathbf{f} = (\sin(u), \cos(u))^T$

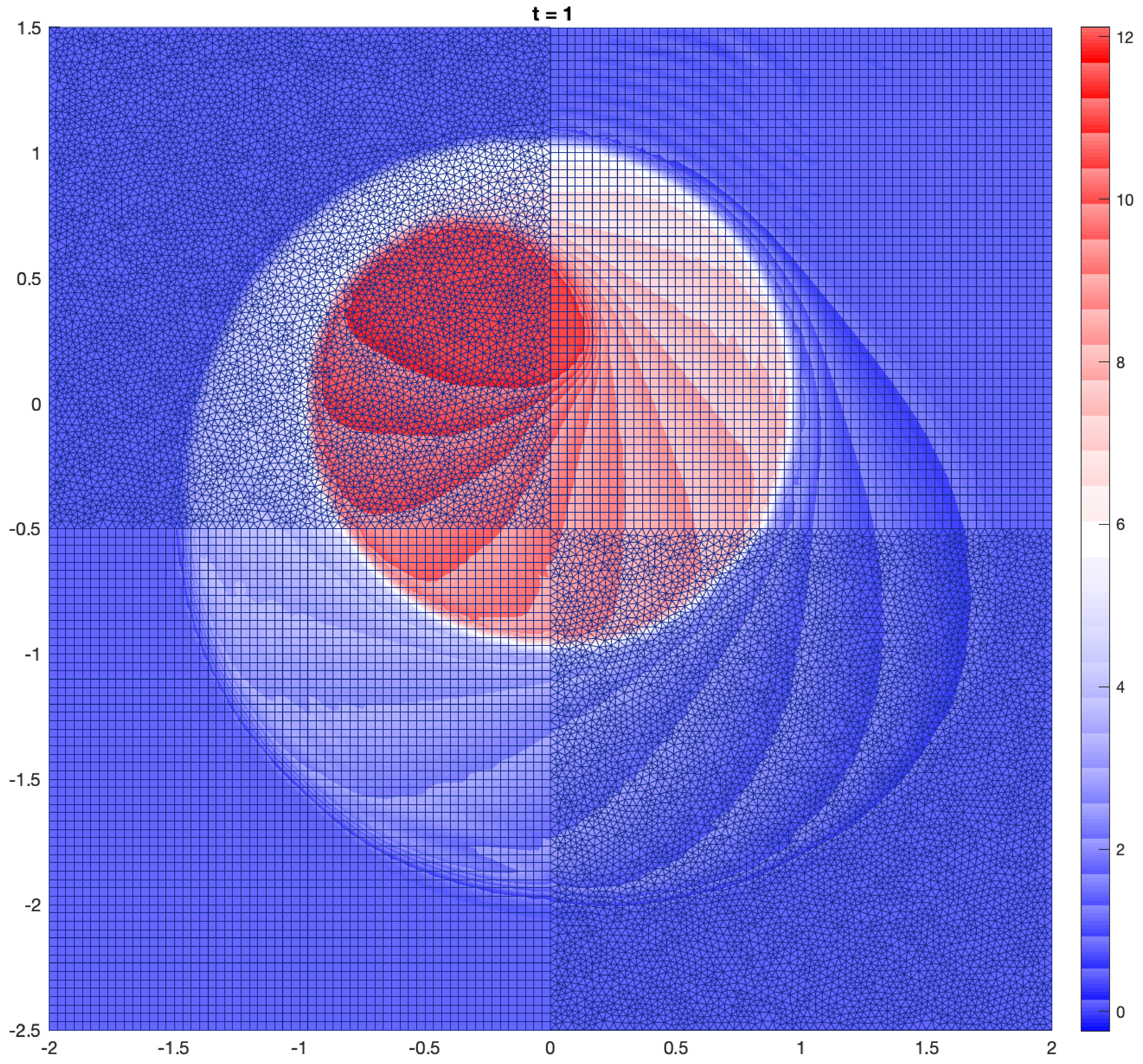

$\mathbf{u}$

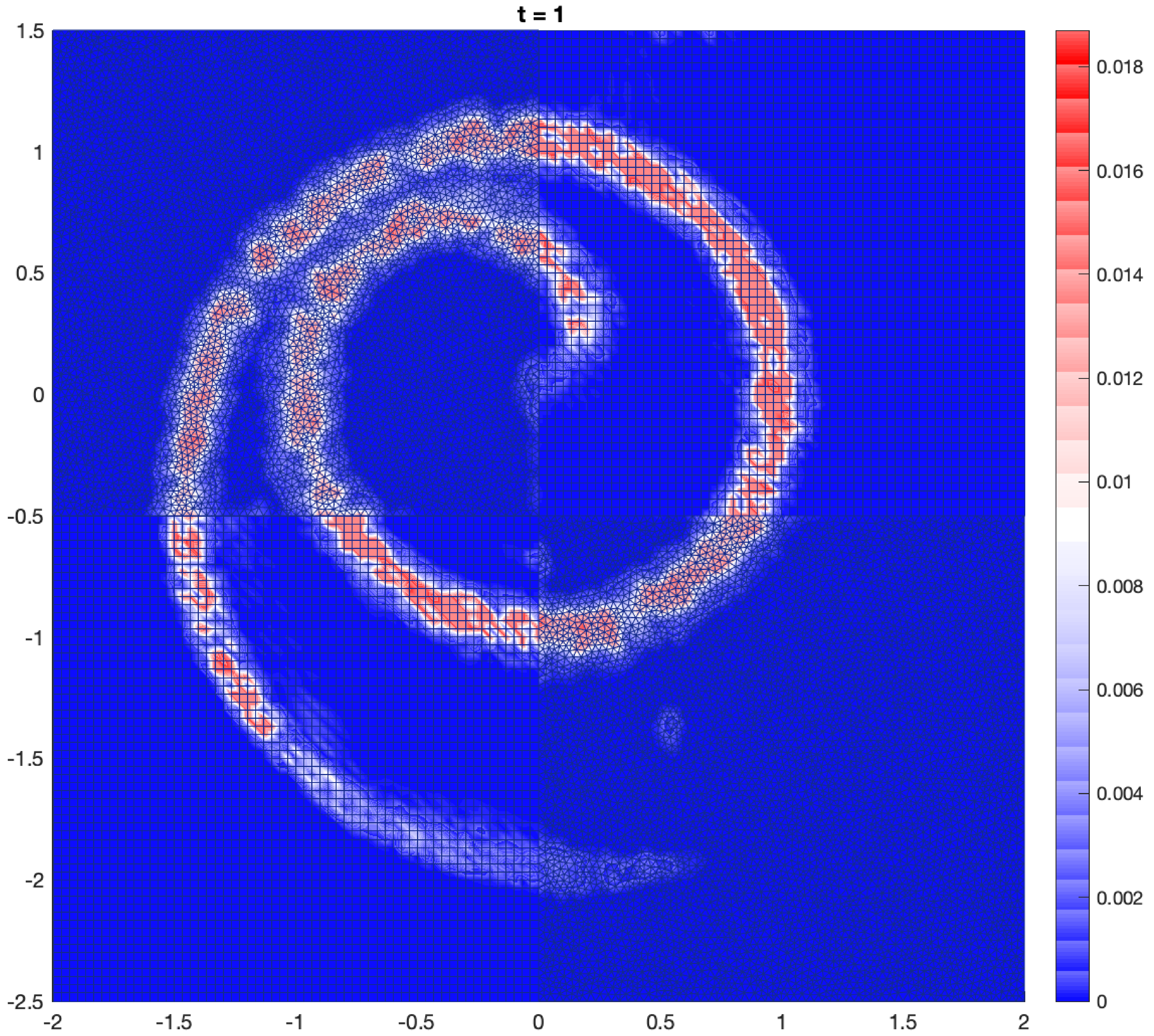

ε_a

Numerical results - The KPP problem

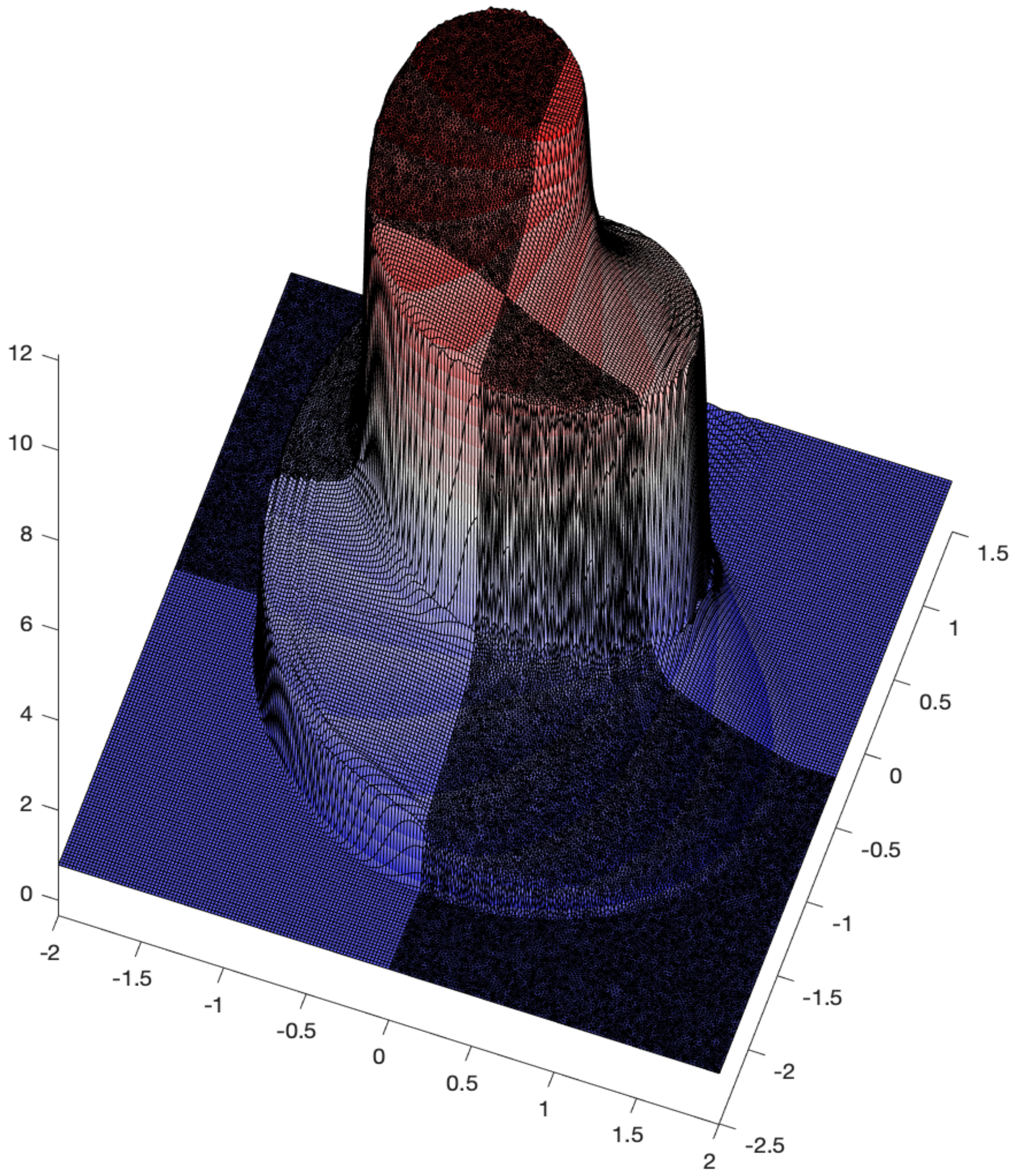

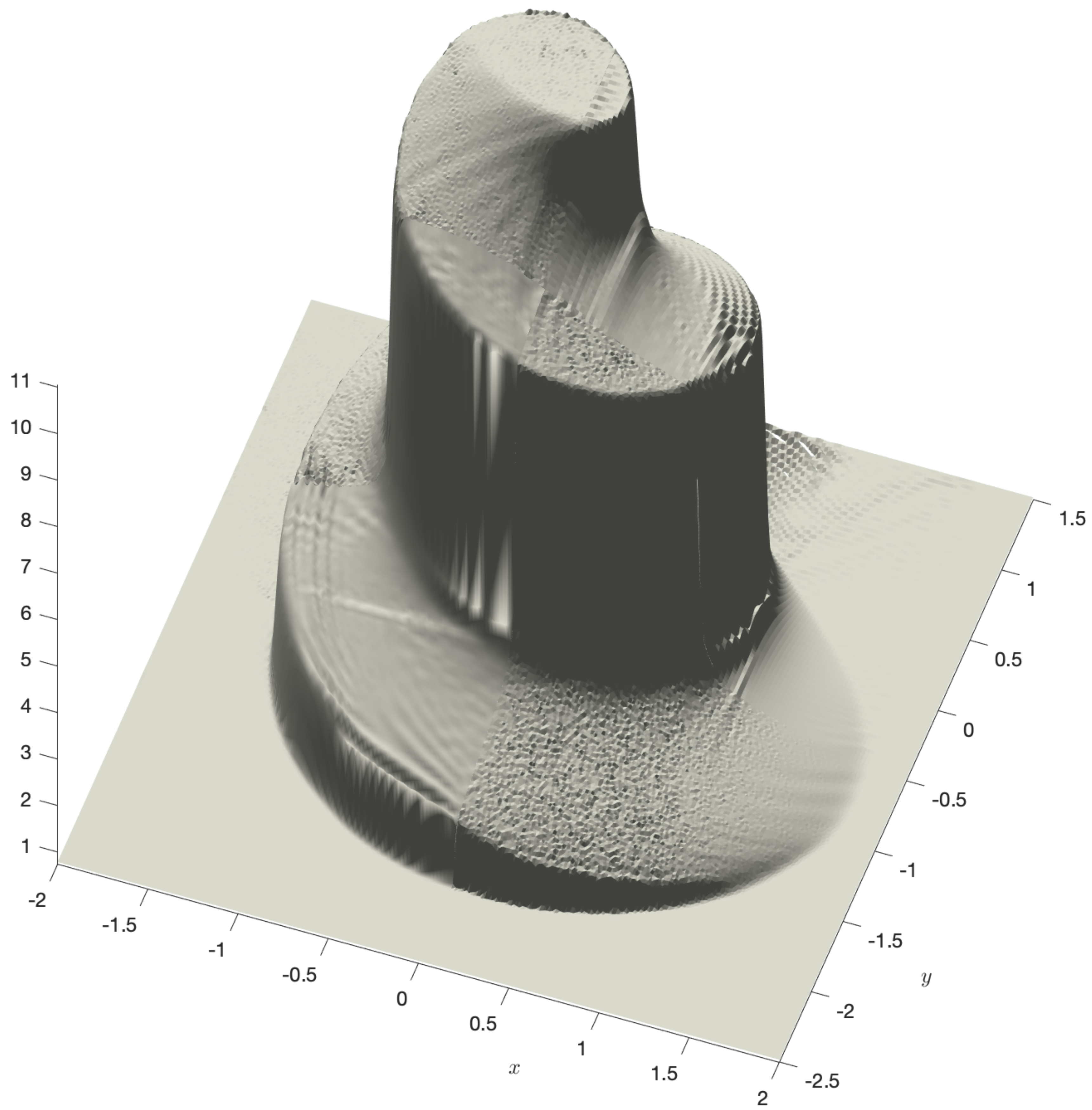

Conclusion

- SBP-SAT framework
- SAT to impose the interface continuity condition
- SBP-preserving interpolation operators to resolve the nonconforming distribution
- Accuracy, stability and conservation are shown
- Minimal modifications to the existing schemes
- Minimal communication between methods
- Preserve FE superconvergence
- Applicable for other conservation laws

Future works

- Curvilinear grids
- Optimal time-stepping
- Upwind operators
- Block corners are not matching
- Systems
- Invariant domain stabilization
- $\mathbb{P}3, \mathbb{P}5$ FE

Thank you for listening!